

# Chemical Inhibitors of a Selective SWI/SNF Function Synergize with ATR Inhibition in Cancer Cell Killing

Emma J. Chory, Jacob G. Kirkland, Chiung-Ying Chang, Vincent D. D'Andrea, Sai Gourisankar, Emily C. Dykhuizen, and Gerald R. Crabtree\*



Cite This: *ACS Chem. Biol.* 2020, 15, 1685–1696



Read Online

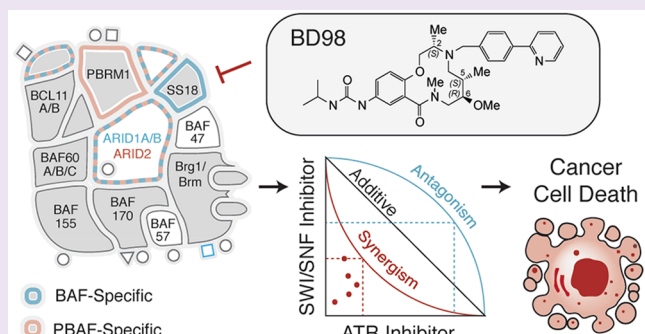
ACCESS |

Metrics & More

Article Recommendations

Supporting Information

**ABSTRACT:** SWI/SNF (BAF) complexes are a diverse family of ATP-dependent chromatin remodelers produced by combinatorial assembly that are mutated in and thought to contribute to 20% of human cancers and a large number of neurologic diseases. The gene-activating functions of BAF complexes are essential for viability of many cell types, limiting the development of small molecule inhibitors. To circumvent the potential toxicity of SWI/SNF inhibition, we identified small molecules that inhibit the specific repressive function of these complexes but are relatively nontoxic and importantly synergize with ATR inhibitors in killing cancer cells. Our studies suggest an avenue for therapeutic enhancement of ATR/ATM inhibition and provide evidence for chemical synthetic lethality of BAF complexes as a therapeutic strategy in cancer.



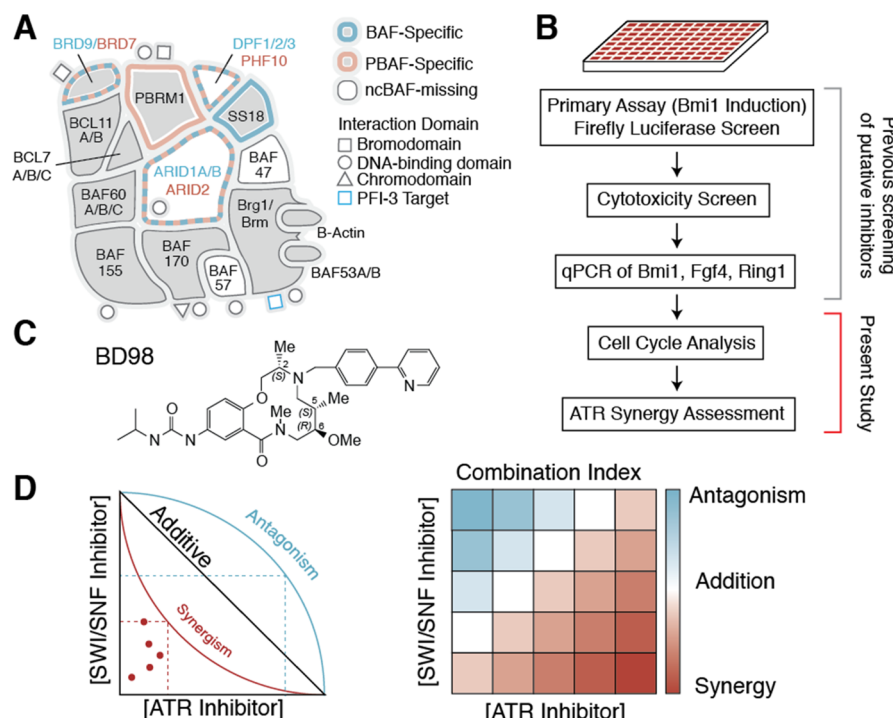


**Figure 1.** Strategy for assessing hypersynthetic lethality of combination BD98 and ATRi. (A) Macromolecular assembly of SWI/SNF complexes. BAF/PBAF-specific subunits labeled in blue/red, respectively. (B) Workflow of screen used to identify putative BAF inhibitors. (C) Structure of BD98. (D) Summary of results (combination index scores, normalized isobolograms) obtained in Chou–Talalay method for assessment of synergy.

frame into the *Bmi1* locus in mESCs, we screened for molecules that could specifically de-repress its expression (Figure 1B).<sup>29</sup> This strategy had the particular advantage of being able to selectively screen for BAF functionality orthogonal to the ATPase function, which would likely result in high levels of toxicity or even oncogenesis. We identified multiple 12-membered macrolactam candidates from a library of diversity-oriented-synthesis molecules<sup>30,31</sup> (Figure 1C) that appear to bind to ARID1A-specific complexes.<sup>32</sup> We find that these inhibitors are remarkably nontoxic in most cell lines and do not appear to independently produce the full decatenation checkpoint arrest found with deletion or depletion of essential subunits such as BRG1 (SMARCA4), BAF57 (SMARCE1), or BAF53a (ACT6LA).<sup>32</sup> This class of structures appears to bind to complexes containing homologous BAF250a/b (ARID1A/B) subunits, which play critical but redundant roles in mammalian BAF function and are specific to canonical-BAF complexes<sup>33</sup> (Figure 1A). Because deletion of *Arid1a/b* in mESCs is lethal yet BD98 produces no toxicity in these cells, it is clear that BD98 is more selective than a total loss of both *Arid1a* and *Arid1b*.

The decatenation checkpoint arrest observed upon deletion of essential subunits of the BAF complex appears to be related to the inability of topoisomerase IIa (TOP2A) to bind to DNA and relieve catenated chromosomes at mitosis.<sup>18</sup> This results in anaphase bridges and cell cycle arrest mediated by ATR (ataxia-telangiectasia mutated and rad3-related protein kinase).<sup>34,35</sup> We also found that this macrolactam class of SWI/SNF inhibitory molecules de-repress the integrated HIV long terminal repeat (LTR), reversing HIV latency.<sup>32,36</sup> This observation led us to determine whether these inhibitors of the repressive function of BAF may provide a therapeutic strategy for cancer without resulting in broad toxicity, as would be expected from BRG1/BRM ATPase inhibitors. Recently,

inhibitors of the ATR kinase demonstrated enhanced chemotoxic effects of DNA damaging agents.<sup>37,38</sup> ATR and ATM are known to phosphorylate BAF170 (SMARCC2) and BRG1 and induce the localization of these complexes to sites of DNA damage.<sup>21</sup> In addition, potent small molecule inhibitors of ATR have been shown to induce a synthetic lethal function in cancer cell lines depleted of the ARID1A/B subunits of the BAF complex.<sup>32</sup> This synthetic lethal interaction has been attributed to the increased dependency of ARID1A/B-deficient cells on the ATR-mediated G2/M decatenation checkpoint following loss of ARID1A/B-mediated interactions of the BAF complex with TOP2A.<sup>18,39</sup> These results suggested that ATR and SWI/SNF inhibition might functionally synergize because they work on contingent steps.<sup>39</sup> To address the potential of BAF-inhibitory molecules to target a highly specific, non-essential function of ARID1A/B, we developed a high-throughput Chou-Talalay method of synergy assessment (Figure 1D), to demonstrate a synergistic, chemical-synthetic lethality in cancers containing canonical BAF complexes, when SWI/SNF and ATR inhibitors are combined. Our data indicate that the use of selective, nontoxic BAF inhibitors might provide a strategy for enhancement of chemotherapeutics in cancer.

## ■ RESULTS AND DISCUSSION

## SWI/SNF Inhibition Sensitizes Cancer Cells to ATR

**Inhibition.** We recently reported a medium-throughput screen in mouse embryonic stem cells (mESCs) to identify small molecules that result in increased expression of *Bmi1*, a known genetic target of BAF whose expression is increased about 10-fold upon deletion or within 60 min of degradation of the *Smarca4* subunit of the BAF complex.<sup>31,40</sup> Through the development of a high-throughput *Bmi1* luciferase reporter assay, we identified multiple 12-membered macrolactam candidates from a library of diversity-oriented-synthesis

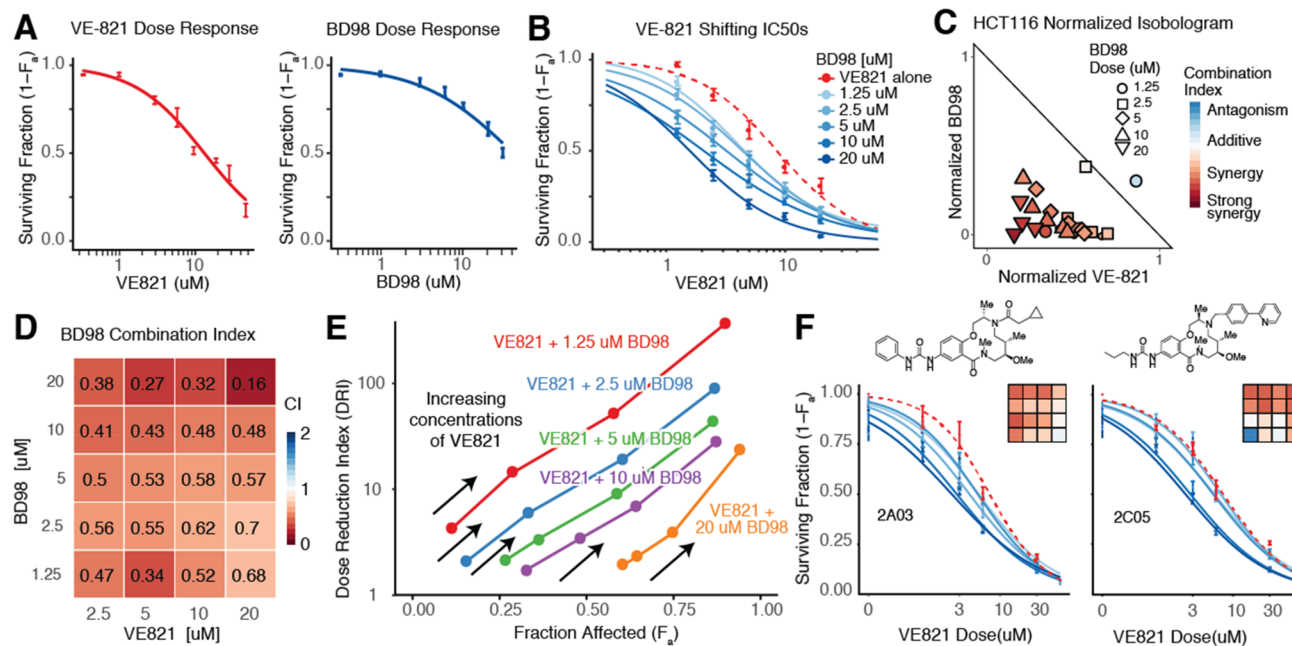


**Figure 2.** BAF and ATR inhibition is synergistic. (A) Dose–response curves of HCT116 cell line exposed to increasing concentrations of ATR inhibitor (VE-821) and putative BAF inhibitor (BD98) for 5 days. (B) Shifting  $IC_{50}$  dose–response curves of HCT116 cells treated with VE-821 and increasing doses of BD98 for 5 days. (C) Normalized isobogram of synergy between VE-821 and BD98 in HCT116 cells. (D) Combination index values quantify synergy between BD98 and VE-821. (E) Plot of the dose reduction index of increasing concentrations of VE-821 and 5 concentrations of BD98 against the fraction of affected cells. (F) Structures, shifting dose response, and CI grid of putative inhibitors demonstrating synergism, 2A03 and 2C05, following treatment with increasing doses of VE-821 (1–30  $\mu$ M) and increasing doses of each putative inhibitor (1–30  $\mu$ M) for 5 days.

molecules<sup>30</sup> that exhibited stereospecificity and provided insight into a structure–activity relationship.<sup>32</sup> Our original *Bmi1* screen also yielded many structurally dissimilar compounds that induced *Bmi1* and *Ring1a* expression with varying degrees of toxicity (as measured by G2/M arrest) (Supplemental Figure 1A,B), suggesting that many initial hits may be disrupting different SWI/SNF related mechanisms<sup>18</sup> or may be nonspecific *Bmi1* activators. Thus, we selected one of the most potent but nontoxic molecules, BRD-K98645985 (which we refer to as BD98) (Figure 1C) for further analysis for synergy with the ATR inhibitor VE-821 on the viability of cancer cells with canonical BAF complexes. We have previously shown that BD98 is able to selectively bind and thermostabilize ARID1A/B *in vitro*,<sup>32</sup> enrich BAF subunits ARID1A, BAF155, PBRM1, and BAF47 by small-molecule pull-down, and activate *Bmi1* at an  $EC_{50}$  of  $\sim 2.4 \mu$ M.<sup>32</sup> Hence, we loosely refer to it as a BAF inhibitor although its direct binding target has not been identified. Because *Arid1a* is essential in mESCs, yet BD98 is nontoxic (Supplementary Figure 1A), we know that BD98 must inhibit a highly selective function of *Arid1a/b* if it is indeed the target of BD98. Previous studies showed that upon acute deletion of *Arid1a*, the  $IC_{50}$  of the ATR inhibitor VE-821 in HCT116 colorectal cancer cells shifted from  $\sim 10$  to  $\sim 1 \mu$ M after 5 days of treatment.<sup>39</sup> In this study, we treated HCT116 cells with increasing doses of VE-821 (1–50  $\mu$ M) and increasing doses of BD98 (1–30  $\mu$ M) independently for 5 days to establish the respective dose responses of the two (Figure 2A). Then, cells were treated with all possible combinations of 5 doses of both VE-821 (1.25–20  $\mu$ M) and BD98 (1.25–20  $\mu$ M) for a total of 25 total combinations in 8 replicates (Figure 2B). By simultaneously treating HCT116 cells with increasing concentrations of VE-821 and the putative BAF inhibitor, BD98, we observed dose-

responsive decreases in VE-821  $IC_{50}$  values ranging from  $\sim 4 \mu$ M at the lowest dose of BD98 (1.25  $\mu$ M) to  $IC_{50} \approx 1 \mu$ M at the highest dose tested in combination (Figure 2B). This indicated that co-inhibition of both BAF and ATR could phenocopy the VE-821-dependent dose responsive shift previously observed by ARID1A knockout in HCT116 cells.<sup>39</sup>

#### Combination BD98/ATR Treatment Is Synergistic.

Occasionally, combining two drugs that act on contingent steps will result in enhanced potency. To assess whether the combined effect is greater than the predicted individual potencies, and hence truly synergistic, requires a rigorous quantitative analysis of both the independent and combined effects of the two molecules through the generation of isobograms and quantification of a combination index (Figure 1D). Synergism in drug combinations allows for the use of lower doses of both molecules, which can reduce adverse effects. Thus, we first aimed to validate the combination of VE-821 and BD98 for synergistic therapeutic value. To assess drug synergy, the Chou–Talalay method was employed to provide a mechanism-independent method to quantify the synergism of drug interactions.<sup>41</sup> This method combines elements of the Scatchard, Michaelis–Menten, Hill, and Henderson–Hasselbalch equations through the law of mass action<sup>42,43</sup> to generate a statistical and quantifiable assessment of synergy. VE-821 and BD98 were tested both independently and then in 25 different combinations in HCT116 cells for 5 days as described above. A combination index (CI), which is a statistically significant representation of synergy, was determined by generating a median-effect equation for each molecule from their respective dose responses. The median-effect equation was used to calculate a median-effect dose for combinations that fell within the linear median-effect range (2.5–20  $\mu$ M). ( $D_x$ )<sub>ATRi, BD98</sub> values,

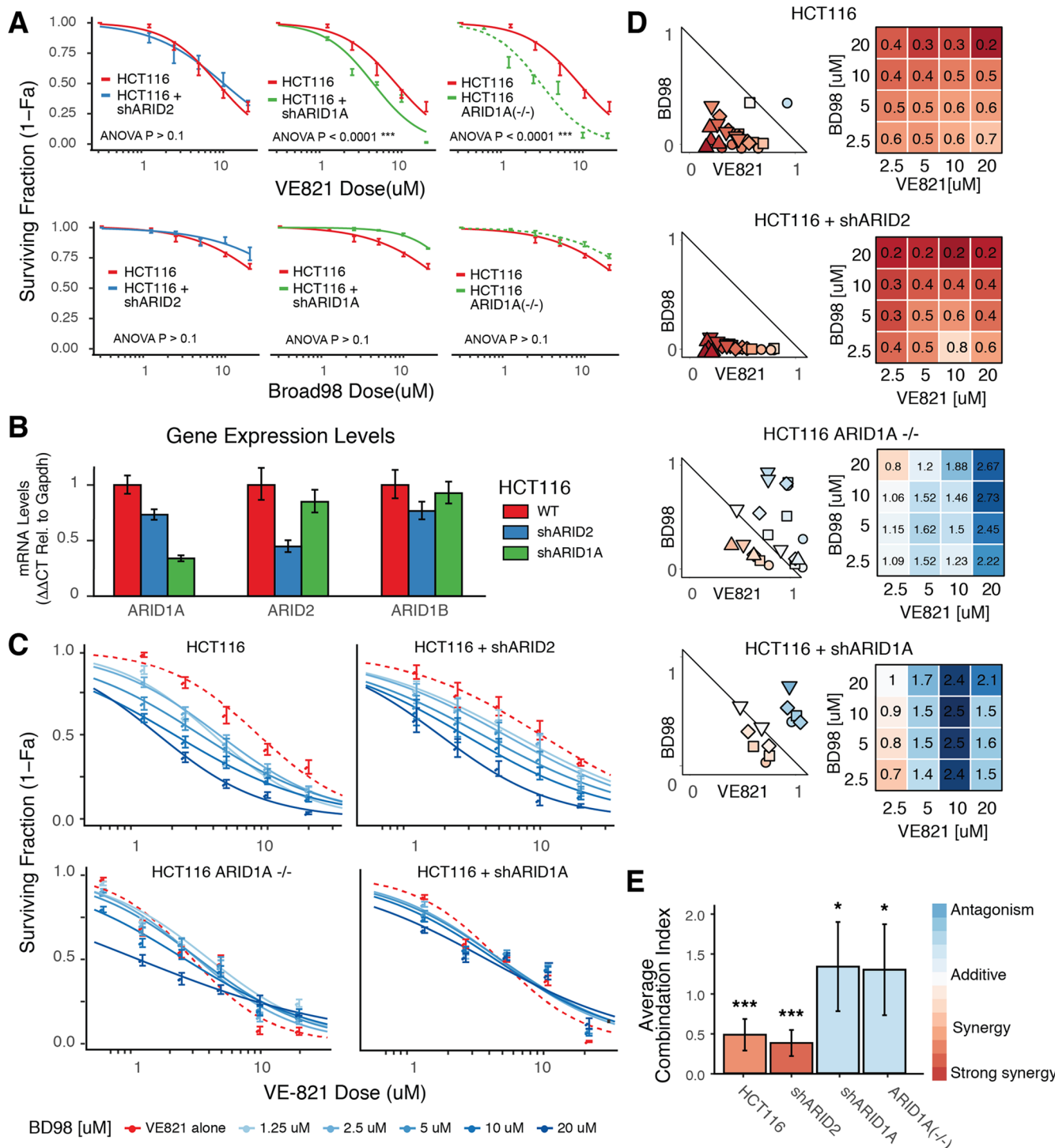


**Figure 3.** Putative BAF inhibitor, BD98, phenocopies knockdown of ARID1A. (A) Cell survival data from HCT116 cells infected with shRNA lentivirus targeting ARID2 (blue), ARID1A (green), control (red), and ARID1A<sup>-/-</sup> HCT116 cells (green-dashed). Following lentiviral transduction and selection, cells were exposed to VE-821 (top) or BD98 (bottom) for 5 continuous days. Error bars represent SD of eight technical replicates in three separate experiments in 384-well plates. ANOVA statistics are reported. (B) Gene expression of ARID1A, ARID2, and ARID1B in HCT116 (WT, shARID1A, shARID2). Delta-Delta CT values compared to GAPDH and ARID1A<sup>+/+</sup> HCT116 cells. (C) Shifting IC<sub>50</sub> plot of ARID1A<sup>+/+</sup> HCT116 cells, ARID1A<sup>-/-</sup> HCT116 cells, and HCT116 cells infected with shRNA lentivirus targeting ARID2 or ARID1A treated with VE-821 and increasing doses of BD98 for 5 days. (D) Normalized isobologram plots of ARID1A<sup>+/+</sup> HCT116 cells, ARID1A<sup>-/-</sup> HCT116 cells, and HCT116 cells infected with shRNA lentivirus targeting ARID2 or ARID1A (as treated in panel C). (E) Average combination indexes for HCT116 cells infected with shRNA lentivirus targeting ARID2, ARID1A, ARID1A<sup>+/+</sup>, and ARID1A<sup>-/-</sup> HCT116. (\*\*\* indicates  $p$ -value < 0.0005, \* indicates  $p$ -value < 0.01 compared to the null hypothesis.).

which correspond to the respective doses of the BD98 and ATRi that correlate with a given percentage of cells affected by

the individual treatments, were also calculated. Normalized index values ( $I_{ATRi}$ ,  $I_{BD98}$ ) and the combination index values (a

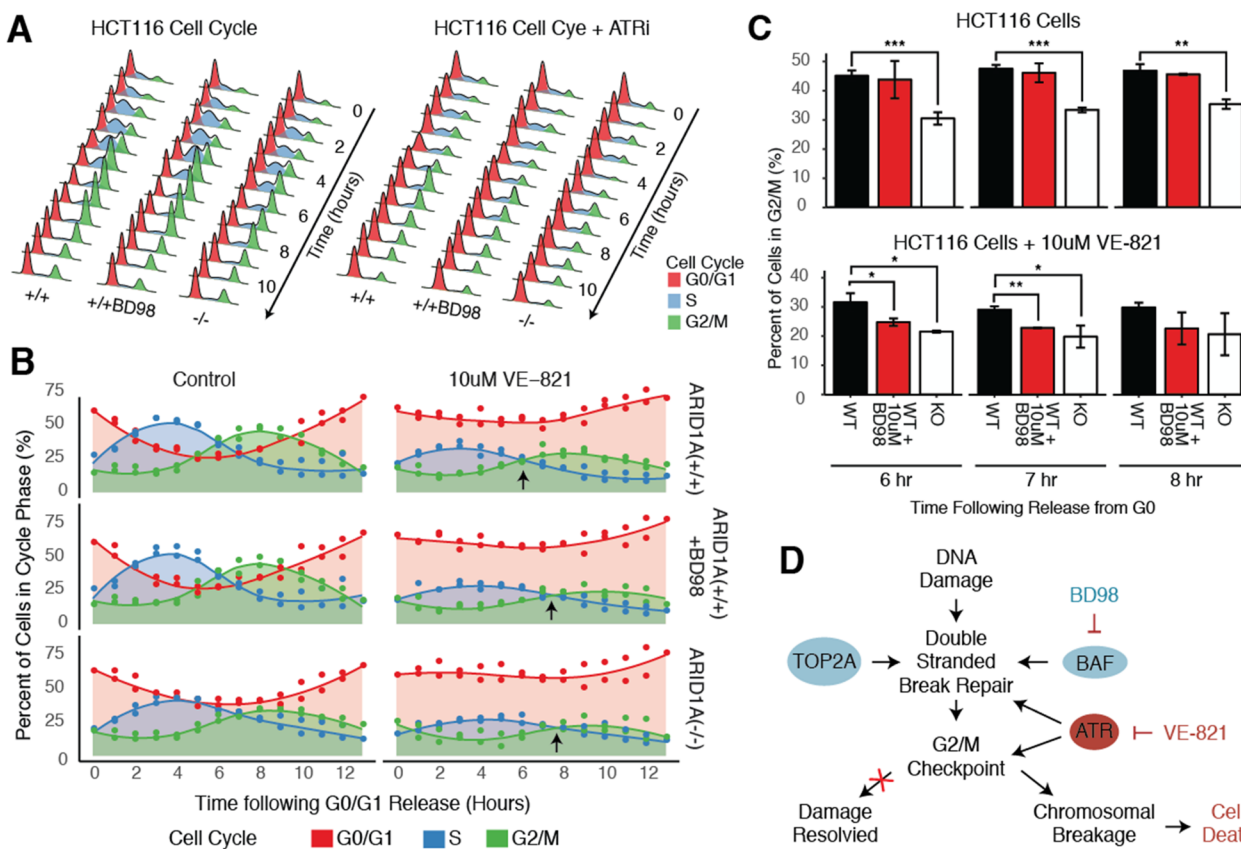


**Figure 4.** BD98 inhibition results in cell cycle defects and is exacerbated by DNA damage. (A) Representative histograms of the cellular propidium iodide-stained DNA content determined by FACS in HCT116 *ARID1A*<sup>+/+</sup>, *ARID1A*<sup>-/-</sup>, and *ARID1A*<sup>+/+</sup> treated with 10  $\mu$ M of BD98 at the indicated time points following release from cell synchronization in G0/G1, in the absence (left) or presence of 10  $\mu$ M VE-821 (right). Time points begin at maximum G0/G1 of second division following release from thymidine block (10 h after release). (B) Time course illustrating the percentage of cells in G0/G1 (red), S (blue), or G2/M (green) phase of synchronously growing HCT116 cells (as treated in panel A). (C) Percent differences of *ARID1A*<sup>-/-</sup> or BD98 treated cells in G2 6, 7, or 8 h after release from G0, as compared to *ARID1A*<sup>+/+</sup> (\*\*p-value < 0.0001, \*\*p-value < 0.001, \*p-value < 0.01). (D) Model of BD98/ATRi induced hypersynthetic lethality mechanism and sensitivity to DNA damage response.

ratio between the treatment dose and the  $D_x$  for a given fraction of affected cells) were then obtained. A combination index of 1 indicates a strictly additive effect, where values less than 1 are synergistic and those greater than 1 are antagonistic. Isobolograms and combination index plots were generated for the tested dose combinations of VE-821 and BD98 (Figure 2C,D). The average combination index observed in HCT116 cells was  $0.53 \pm 0.05$ , which indicates clear synergy between VE-821 and BD98 (Figure 2D). Further, the dose reduction index (an inverse relation to the combination index) was calculated to demonstrate that at low concentrations, the combination of VE-821 and BD98 can reduce the dosing over 10-fold, while at higher concentrations of VE-821, the dose reduction index reaches nearly 100 (Figure 2E), indicating that the combination has the potential to significantly lower the dosing of the toxic ATR inhibitor.

We have published an analysis of striking stereospecificity of the BD98 related molecules,<sup>32</sup> so we also sought to assess whether any additional molecules from our primary screen would phenocopy ATRi sensitivity. Thus, synergy was assessed for 8 additional hits from our primary screen with VE-821, as described above. We observed that two structurally similar molecules (2A03 and 2C05) indeed demonstrated comparable synergy with VE-821 in HCT116 cells ( $CI_{2A03} = 0.65 \pm 0.05$ ,  $CI_{2C05} = 0.69 \pm 0.08$ ) (Figure 2F). However, the administration of all other compounds tested resulted in either

additive or antagonistic effects when combined with VE-821 (Supplemental Figure 1C). Interestingly, the published PFI-3 BRG1-bromodomain inhibitor showed no measurable dose-responsive or synergy effects in the *ARID1A*<sup>+/+</sup> or *ARID1A*<sup>-/-</sup> HCT116 cell lines (Supplemental Figure 1C,D), suggesting that inhibition of the acetyl-lysine-binding function of the BRG1/BRM/PBRM1 subunits is not the major mechanism through which synergy is observed. These studies underlie the specificity of the action of the structurally related SWI/SNF inhibitors compared to other hits that similarly induce gene de-repression (Supplemental Figure 1B).<sup>29,32</sup>

**BD98 Phenocopies Selective Features of ARID1A/B Loss.** To analyze the effects of ARID1A on the synergistic combination, we made use of HCT116 cells for which we have both isogenic *ARID1A*<sup>+/+</sup> and *ARID1A*<sup>-/-</sup> cell lines. The *ARID1A*<sup>-/-</sup> line contains the homozygous mutation p.Q456\*/p.Q456\*. The primary target of our original screen (*Bmi1*) is induced by loss of SMARCA4, which is present in human BAF, PBAF, and ncBAF complexes<sup>5,33</sup> (Figure 1A). PBAF complexes differ from BAF complexes by incorporation of orthogonal subunits, specifically, ARID2 (as opposed to ARID1A/B), PHF10 (BAF45a) (as opposed to DPF10/BAF45d), and PBRM1 (Figure 1A). PBAF-specific subunits are also frequently mutated in cancer, specifically renal clear cell carcinomas and cholangiocarcinomas.<sup>44–47</sup> To narrow whether BD98 is acting on BAF or PBAF-related pathways, we

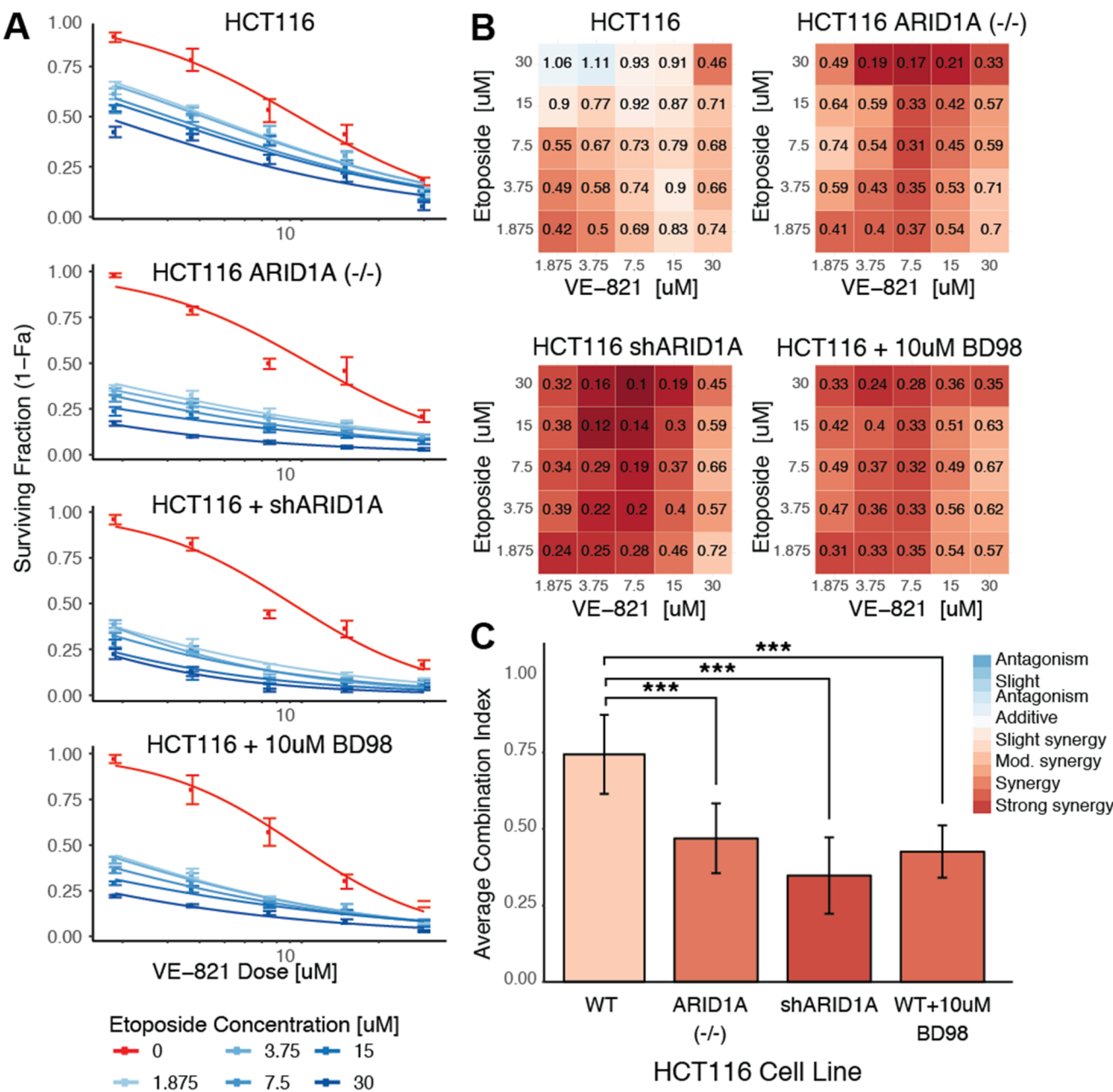


**Figure 5.** Sensitivity of ARID1A deficient cells to VE-821 and etoposide. (A) Shifting dose responses of  $ARID1A^{+/+}$  HCT116 cells,  $ARID1A^{-/-}$  HCT116, shARID1A cells, and  $ARID1A^{+/+}$  HCT116 cells treated with BD98, following 5-days of treatment with 25 dose combinations of VE-821 and etoposide. (B) Combination index grids of cell lines (as treated in panel A). (C) Average combination indexes for HCT116 treated with etoposide and VE-821 (as treated in panel A). \*\*\* $p$ -value < 0.0001.

constitutively knocked down ARID1A or ARID2 by lentiviral transduction of  $ARID1A^{+/+}$  HCT116 cells and compared the BD98/ATRi synergy to  $ARID1A^{+/+}$  and  $ARID1A^{-/-}$  cells. Knockdown shARID1A cells demonstrated increased sensitivity to VE-821 as expected, as did the homozygous loss-of-function  $ARID1A^{-/-}$  HCT116 cell line. In contrast, shARID2 cells responded to ATR treatment similarly to  $ARID1A^{+/+}$  cells (Figure 3A). Importantly, upon knockdown of ARID1A or ARID2 (Figure 3B), the synergistic effect observed between BD98 and VE-821 was only ablated upon loss of ARID1A (Figure 3C–E) ( $CI_{shARID1A} = 1.48 \pm 0.14$ ,  $CI_{ARID1A(-/-)} = 1.44 \pm 0.12$ ), but not loss of ARID2 ( $CI_{shARID2} = 0.42 \pm 0.04$ ) (Figure 3D,E). This suggests that in the context of colorectal cancer, BD98 is acting through ARID1A-dependent mechanisms or specific subunits or functions of such complexes.

Additionally, both shARID1A and  $ARID1A^{-/-}$  cells were slightly but not significantly less sensitive to BD98 than  $ARID1A^{+/+}$  HCT116 cells (Figure 3A). This minor effect is likely because ARID1A is partially redundant with ARID1B in colon cancer but could also be related to an off-target effect independent of ARID1 proteins.

**ATRi/BD98 Inhibition Results in Cell Cycle Defects.** Given that we find that BD98 is largely nontoxic in mESCs, we next sought to understand the mechanism by which BD98 kills cells in the presence of ATR inhibitors. To investigate this, we synchronized HCT116 cells in the early G1/S phase and then tracked their progression through the cell cycle upon release into media containing BD98. To assess the full cell cycle, time

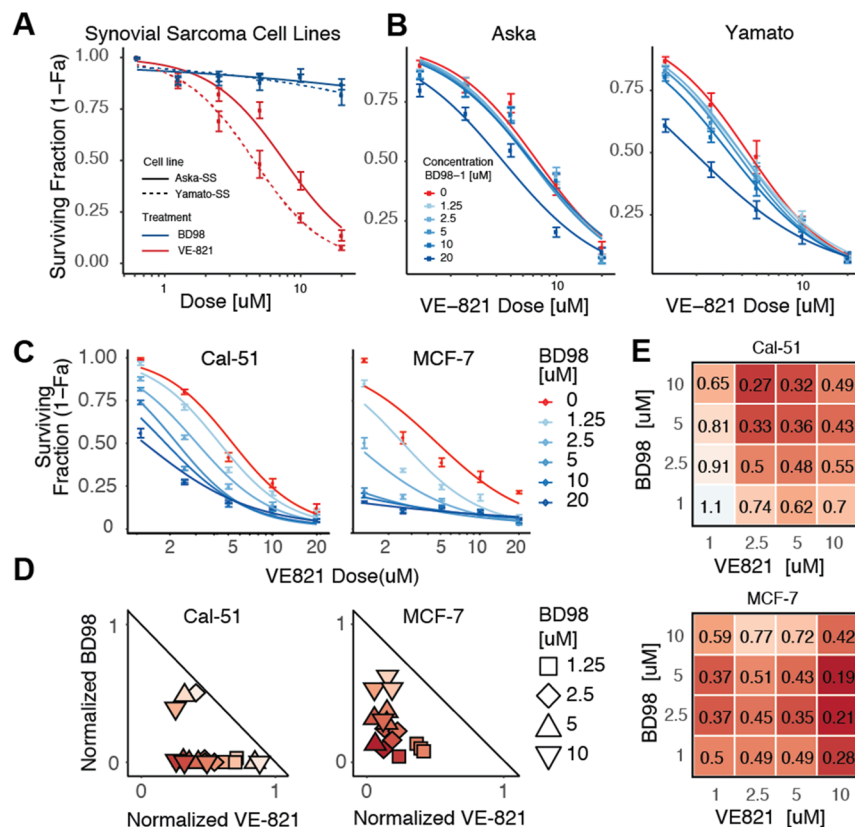


**Figure 6.** BD98 sensitization in additional SWI/SNF mutant cell lines. (A) Dose responses of synovial sarcoma cell lines treated with VE-821 or BD98. (B) No observable shifting dose response curves of synovial sarcoma cell lines treated with increasing combinations of VE-821 and BD98. (C) Shifting dose response curves of Cal-51 and MCF7 cell lines treated with increasing combinations of VE-821 and BD98. (D) Normalized isobolograms of Cal-51 and MCF7 cell lines treated with increasing combinations of VE-821 and BD98. (E) Combination index plots of Cal-51 and MCF7 cell lines treated with increasing combinations of VE-821 and BD98.

points were collected beginning at early G0/G1 of the second cell division following release from thymidine block. We observed that *ARID1A*<sup>-/-</sup> HCT116 cells exhibited slightly delayed progression through S-phase compared to both acutely BD98 treated (10  $\mu$ M) and untreated *ARID1A*<sup>+/+</sup> HCT116 cells but overall progressed through the cell cycle at similar rates (~11 h per cycle) (Figure 4A,B). This is consistent with our observation that BD98 independently has minimal toxicity or effects on proliferation. We were curious as to the mechanism by which BD98 in combination with ATRi kills cells, so we further tracked the progression of cells released into media containing VE-821 (10  $\mu$ M) in the presence or absence of BD98 compared to *ARID1A*<sup>-/-</sup> cells under the same conditions (Figure 4B). Consistent with previous results, we observed that HCT116 *ARID1A*<sup>-/-</sup> cells displayed delayed progression through S phase, which is exacerbated by ATRi through relief of the pile-up leading to premature entry into mitosis (Figure 4A,B).<sup>39</sup> In addition, when treated with 10  $\mu$ M BD98 in combination with VE-821, *ARID1A*<sup>+/+</sup> HCT116 cells similarly exhibited delayed progression through S phase (Figure 4B,C), comparable to *ARID1A* knockout. This result suggests that delayed progression through S phase as a result of BD98 is likely due to either an inability of *ARID1A*-containing complexes to repair DNA damage or perhaps collapsed or stalled replication forks, which result from defective function of the BAF complex.<sup>48</sup> Unsurprisingly, we observed that there is little difference in whole cell DNA damage between *ARID1A*<sup>+/+</sup> and *ARID1A*<sup>-/-</sup> HCT116 cells (Supplemental Figure 2A) since these cells behave comparably in the absence

of ATRi treatment. Thus, we turned to mouse embryonic stem cells (mESCs) for acute deletion of BAF complex subunits. As deletion of both copies of *Brg1* in mESCs results in anaphase bridges and inviability,<sup>18</sup> we acutely deleted a single copy of *Brg1* in mESCs and observed an increase in both medium and high amounts of DNA breaks (Supplemental Figure 2B). This increase in DNA breaks with depleted levels of the ATPase may explain the heightened synergistic effect observed in the presence of ATRi (Figure 4D).

**SWI/SNF Inhibitor Effects Are Exacerbated by DNA Damage.** Recent studies have indicated a role of SWI/SNF remodeling complexes in DNA damage repair through either ATR/ATM-dependent phosphorylation of BAF170, which recruits BAF to double stranded break (DSB) repair sites<sup>21,48</sup> or through resolving DNA decatenation through a direct interaction with TOP2A.<sup>18</sup> Previously, it was reported that knockdown of TOP2A in *ARID1A*<sup>-/-</sup> HCT116 cells resulted in high levels of cell death, which was presumed to be a result of a stronger dependency on TOP2A upon loss of *ARID1A*.<sup>39</sup> To assess the mechanism of ATR-dependent BAF sensitivity in cancer cells and whether it was truly TOP2A-dependent, synergy was assessed between VE-821 and TOP2A/B inhibitors in *ARID1A*<sup>+/+</sup> and *ARID1A*<sup>-/-</sup> HCT116 cells. Both cell lines were treated with increasing doses of the TOP2A inhibitor etoposide and the TOP2B inhibitor XK469<sup>49</sup> for 5 days (Supplemental Figure 3A) with increasing doses of VE-821 (Figure 5A, Supplemental Figure 3B), and the synergy between them was calculated (Figure 5B,C, Supplemental Figure 3C). Modest synergy was observed when both

*ARID1A*<sup>+/+</sup> and *ARID1A*<sup>-/-</sup> cells were treated with the TOP2B inhibitor ( $CI_{XK469(+/-)} = 0.75 \pm 0.05$ ,  $CI_{XK469(-/-)} = 0.85 \pm 0.09$ ) (Supplemental Figure 3C). In contrast, in the *ARID1A*<sup>+/+</sup> cells, VE-821 and etoposide demonstrated moderate synergy, but “strong synergy” was observed upon *ARID1A* knockout and knockdown (Figure 5B,C) and importantly upon treatment with 10  $\mu$ M BD98. In all three cases of deletion, knockdown, and chemical inhibition, loss of *ARID1A* functionality resulted in statistically stronger responses to coadministration of TOP2A and ATR inhibition ( $p$ -value < 0.0001). This suggests that in the absence of functional canonical BAF complexes, by either chemical or genetic deletion, cancer cells may be unable to repair DSBs, which results in rapid cell death following checkpoint bypass due to ATR inhibition.

**BAF Inhibition in Mutant SWI/SNF Cell Lines.** In *ARID1A*-deficient tumors, ATR inhibition is thought to trigger premature mitotic entry and chromosome instability that cannot be resolved, resulting in mitotic catastrophe.<sup>39</sup> Recent reports have demonstrated that loss-of-function BRG1 mutations have increased sensitivity to topoisomerase II inhibition in the presence of PRC2 inhibitors<sup>50</sup> and that cancers with oncogenic BAF mutations may also exhibit increased sensitivity to PRC2 inhibition.<sup>51</sup> We sought to assess which cancers, including BAF-deficient cancers, might be susceptible to ATR sensitization by inhibiting SWI/SNF pathways. We tested the efficacy of BD98 and ATRi on six additional human cancer cell lines including two highly mutated proliferative cell lines (Cal-51 and MCF-7), two synovial sarcoma cell lines (Aska, Yamato), which are driven by noncanonical BAF functions (ncBAF), and two renal-cell carcinoma lines (A-704, ACHN), which harbor a mutation in the PBAF-specific subunit PBRM1<sup>45</sup> or are heterozygous mutants for PBRM1, respectively (Supplemental Figure 4). Interestingly, Cal-51 is *ARID1A* null (Supplemental Figure 5A) but appears to be *ARID1B*-dependent, as we were unable to successfully knock down *ARID1B* with well-established knockdown constructs (Supplemental Figure 5B).<sup>52</sup> To assess synergy, each cell line was treated with combinations of 5 doses of VE-821 and 5 doses of BD98 as described above. Both synovial sarcoma cell lines demonstrated no measurable dose-response to BD98 (Figure 6A,B), and no quantifiable synergy between BD98 and VE-821 could be obtained. This supports the evidence that BD98 is likely acting on a canonical BAF pathway, as it has recently been discovered that the proliferation of synovial sarcoma and malignant rhabdoid tumors are dependent on ncBAF complexes, which contain neither *ARID1A* or *ARID1B*, among other subunits (Figure 1A).<sup>33</sup> Interestingly, BD98 sensitized both MCF-7 and Cal-51 cells to ATR inhibition ( $CI_{MCF-7} = 0.45 \pm 0.04$ ,  $CI_{Cal-51} = 0.57 \pm 0.09$ ) (Figure 6C–E), despite the total loss of *ARID1A* in the Cal-51 line. Because Cal-51 cells have biallelic loss of *ARID1A* (Supplemental Figure 5A), the synergy observed in this line most likely results from the actions of the redundant *ARID1B*<sup>6,53</sup> but highlights the nonobvious nature of identifying potential clinical target populations. Finally, in both renal-cell carcinoma lines (ACHN, A-704), the drug combination demonstrated no measurable synergy (Supplemental Figure 5C,D). Together, these results suggest that BD98’s mechanism is acting through an *ARID1*-related pathway.

## ■ DISCUSSION

In this study, we assess whether small-molecule inhibition of a specialized function of canonical BAF complexes can serve as a viable therapeutic strategy for the treatment of cancer. The 15 subunits of BAF complexes are combinatorially assembled from the products of 31 genes giving them remarkable biological specificity.<sup>12,54</sup> This conceptual advance led us to search for inhibitors of the specific repressive function of canonical BAF complexes in the hope of avoiding toxicity, while still targeting a potentially druggable aspect of these large assemblies. Previous work indicated that ATR-induced BAF phosphorylation is essential for localization to sites of DNA damage and that cancer cell lines deficient in BAF complexes exhibit synthetic lethality with a variety of clinical cancer therapeutics.<sup>39,50,55</sup> These observations led us to test the possibility that an inhibitor of a specialized function of BAF complexes might synergize with ATR inhibitors, allowing them to be used at lower, less toxic concentrations in the treatment of cancer. General inhibitors of BRG1/BRM ATPases have been described<sup>27,28</sup> but because the loss of BRG1/SMARCA4 is lethal in nearly all cell types, they are likely far too toxic for therapeutic use. In addition, an inhibitor of the bromodomain of BRG1 has been described, but it is not effective at inhibiting cancer cell growth.<sup>26</sup> By combining BD98 with inhibitors of the ATR kinase, we have demonstrated that cancer cells undergo a chemically induced synthetic lethal effect, particularly in cancers whose oncogenesis is not primarily SWI/SNF-dependent. This suggests that inhibitors of canonical BAF have the potential for broader therapeutic utility, beyond classically disrupted BAF-related cancers such as synovial sarcomas,<sup>56</sup> malignant rhabdoid tumors,<sup>57,58</sup> and renal clear cell carcinomas.<sup>43,47</sup>

Therapeutic targeting of multisubunit complexes has been a challenge due to the varied functions, compositions, and specificity of such complexes. Suspected inhibitors of protein complexes likely lack substrate affinity for a single subunit but rather interact with composite surfaces produced by combinatorial assembly. This poses significant barriers to traditional biochemical characterizations, as demonstrated by our prior efforts to identify the specific target of interaction.<sup>32</sup> Further, challenges surrounding complex purification, along with the lack of high-resolution structural insights into such diverse complexes has kept the development of specific inhibitors largely out-of-reach.<sup>1</sup> Based on previous work<sup>21,39</sup> we reasoned that small molecules that block canonical *ARID1A*-containing BAF complexes may also be synergistic with ATR inhibition. Many of the putative BAF inhibitors that we discovered in our primary screens were highly toxic, as would be expected based on the essential role of most subunits of the BAF complex. However, many specific molecules that block the transcriptional repressive function of BAF complexes appear nontoxic, and yet we show that they are highly synergistic with ATR inhibition in several human cell lines. Of the initial hits that arose from our previous screen,<sup>29,32</sup> we have observed that the macrocyclic candidates exhibited exquisite stereospecificity, which will aid in the development of better and more potent inhibitors of SWI/SNF-dependent pathways. Despite the observation of strong synergy between BD98 and ATRi, challenges remain to transition these compounds into animal models. These macrocyclic inhibitors are synthesized through a nucleophilic aromatic substitution intramolecular ring-forming process with stereochemical dependencies,<sup>59</sup> and

as such, scale-up remains a bottleneck and the limiting quantities of compound can be prohibitive to downstream characterizations. This further highlights the need for early validation assays that require very little compound, such as the synergy method employed in this work.

Our studies and previous observations indicate that the mechanism underlying synergy between BD98 and ATR inhibition is likely related to ATR/ATM phosphorylation of BRG1 and BAF170 promoting the interaction of BAF with sites of DNA damage,<sup>21</sup> which is further exacerbated upon treatment with inhibitors of TOP2A (Figure 5E). Therefore, we hypothesize that synergy of the two inhibitors arises from the roles of ATR in recruiting BAF to sites of DNA damage, BAF-dependent DNA damage repair, and the role of ATR in checkpoint arrest. Failure at each of these contingent steps could lead to synergistic cell death. While acute ARID1A loss has been shown to provide synthetic lethality with ATR inhibition,<sup>39</sup> the role of ATR in the localization of BAF to sites of DNA damage suggest a broader role of BD98 and like molecules in treating cancer other than just cancers that have mutations in ARID1A or ARID1B. This, coupled with recent findings that tumor cells deficient in BAF complexes exhibit synthetic lethality from a variety of chemotherapeutics (anti-PD-1, checkpoint kinase inhibitors, EZH2 inhibitors),<sup>39,50,55</sup> suggests that chemical inhibition of BAF complexes may have synergistic value by sensitizing cancers to a range of therapeutics.

## METHODS

**Cell Culture.** HCT116 ARID1A<sup>+/+</sup> and ARID1A<sup>-/-</sup> cell lines were courtesy of Dr. Diana Hargreaves and originally obtained from Horizon Discovery. Cancer cell lines were obtained from American Type Tissue Collection. All cancer cell lines were grown in McCoy's 5a media supplemented with 10% FBS. mESCs were cultured with standard conditions on gelatin coated plates in DMEM media containing 7.5% FBS, 7.5% serum-replacement, and leukemia inhibitory factor (LIF). Media was replenished daily, and cells were passaged every 48 h. For complete reagents, cell line details, and methods, see *Supplemental Experimental Procedures*.

**Synergy Viability Assays.** Viability assays were performed in 384-well plates. Cells were plated at 500 cells/well. Twenty-five dose combinations were administered 24 h after seeding, and media containing fresh drug was replaced every 48 h. After 5 days, cellular viability was measured and combination index values were calculated utilizing R (Github: EChormatin/SynergyCalc), as described by Chou and Talalay.<sup>43</sup> See *Supplemental Experimental Procedures*.

**Lentiviral Preparation and Infection.** Lentiviruses were produced with LentiX-HEK293T cells via spinfection with polyethylenimine transfection. HEK293T cells were cultured using standard conditions in DMEM media containing 10% FBS. HEK293T cells were transfected with PEI with lentiviral pLKO shARID1A, GIPZ shARID2, and GIPZ shARID1B knockdown vectors and co-transfected with packaging vectors psPAX2 and pMD2.G as previously described.<sup>60</sup> Viral supernatant was collected and used for spinfection. Infected cells were selected with puromycin 48 h following transfection and maintained under selection for 2–3 passages. See *Supplemental Experimental Procedures*.

**RT-qPCR Analysis.** RNA was extracted from cells, cDNA was synthesized, and samples were analyzed by qPCR. See *Supplemental Experimental Procedures* and Supplemental Table 1.

**Cell Synchronization.** HCT116 cells were plated 6-well plates and incubated with thymidine for 18 h, released into fresh media for 8 h, and re-incubated with thymidine again for 16 h, washed several times with PBS, released into fresh media to synchronize into G1/early S, and then collected at respective time points. The mESCs were incubated with thymidine for 8 h, released into fresh media for 7 h,

and then incubated with thymidine again for 7 h. Cells were washed several times with PBS, released into fresh media, and collected at respective time points. See *Supplemental Experimental Procedures*.

**Cell Cycle Analysis.** For hour-by-hour analysis, cancer cells were collected, rinsed with PBS, and fixed in 70% ethanol. Cells were fixed overnight, pelleted, rinsed in PBS, stained with propidium iodide, and analyzed by flow cytometry. For mESCs, cell cycle analysis was performed by staining with bromodeoxyuridine–fluorescein isothiocyanate (BrdU-FITC)/7-aminoactinomycin D (7-AAD) and analyzed by flow cytometry. See *Supplemental Experimental Procedures*.

**Comet Assay.** HCT116 cells and mESCs were dissociated and analyzed with single cell gel electrophoresis. After staining with vista Green DNA dye, comet images were captured by fluorescence microscopy. See *Supplemental Experimental Procedures*.

**Western Blot.** Nuclear extracts were prepared by benzonase treatment in nuclear extract buffer containing HEPES, KCl, EDTA, MgCl<sub>2</sub>, glycerol, NP-40 Protease inhibitors, DTT, and benzonase (See *Supplemental Experimental Procedures* for full details). Nuclei were lysed in radioimmunoprecipitation assay (RIPA) buffer, and protein concentrations were determined by Bradford assay (Biorad). Proteins were separated by SDS–PAGE electrophoresis with a 4–12% Bis-Tris protein gel (Thermo Scientific) and then transferred to an Immobilon-FL membrane (Millipore). Blots were probed with primary antibodies, rabbit  $\alpha$ -Arid1a (D2A8u) (1:1000, Cell Signaling no. 12354) and mouse  $\alpha$ -Arid1b (D2D) (1:1000, Novus Biologicals no. H00057492-M01), followed by fluorescence-conjugated secondary antibodies (Li-Cor), and bands were detected using an Odyssey CLX imaging system (Li-Cor).

## ASSOCIATED CONTENT

### SI Supporting Information

The Supporting Information is available free of charge at <https://pubs.acs.org/doi/10.1021/acschembio.0c00312>.

Synergy analysis among putative SWI/SNF inhibitors, DNA damage in mESCs and HCT116 cells, dose response curves and shifting IC<sub>50</sub> plots of topoisomerase inhibitors, mutations in cancer lines involved in this study, ARID1A/B mutant cancer lines, qPCR primers, and supplemental experimental procedures (PDF)

## AUTHOR INFORMATION

### Corresponding Author

Gerald R. Crabtree – Departments of Developmental Biology and Pathology, Stanford University School of Medicine, Stanford, California 94305, United States; Howard Hughes Medical Institute, Chevy Chase, Maryland 20815, United States;  [orcid.org/0000-0001-9685-7911](https://orcid.org/0000-0001-9685-7911)

### Authors

Emma J. Chory – Department of Chemical Engineering, Stanford University, Stanford, California 94305, United States; Departments of Developmental Biology and Pathology, Stanford University School of Medicine, Stanford, California 94305, United States;  [orcid.org/0000-0001-8541-9289](https://orcid.org/0000-0001-8541-9289)

Jacob G. Kirkland – Departments of Developmental Biology and Pathology, Stanford University School of Medicine, Stanford, California 94305, United States;  [orcid.org/0000-0001-5617-7065](https://orcid.org/0000-0001-5617-7065)

Chiung-Ying Chang – Departments of Developmental Biology and Pathology, Stanford University School of Medicine, Stanford, California 94305, United States;  [orcid.org/0000-0002-2511-0033](https://orcid.org/0000-0002-2511-0033)

Vincent D. D'Andrea – Departments of Developmental Biology and Pathology, Stanford University School of Medicine, Stanford, California 94305, United States

**Sai Gourisankar** — Department of Chemical Engineering, Stanford University, Stanford, California 94305, United States; Departments of Developmental Biology and Pathology, Stanford University School of Medicine, Stanford, California 94305, United States;  [orcid.org/0000-0003-0132-8086](https://orcid.org/0000-0003-0132-8086)

**Emily C. Dykhuizen** — Department of Medicinal Chemistry and Molecular Pharmacology, Purdue University, West Lafayette, Indiana 47907, United States;  [orcid.org/0000-0003-3072-1469](https://orcid.org/0000-0003-3072-1469)

Complete contact information is available at:  
<https://pubs.acs.org/10.1021/acschembio.0c00312>

## Author Contributions

E.J.C. designed and conducted the experiments, analyzed data, and wrote the manuscript. J.G.K., C.Y.C., S.G., and V.D.D. designed and conducted experiments. G.R.C. and E.C.D. designed experiments and wrote the manuscript. All authors assisted with manuscript revisions.

## Notes

The authors declare the following competing financial interest(s): G.R.C. is a scientific co-founder, shareholder, and consultant of Foghorn Therapeutics, Inc.

## ACKNOWLEDGMENTS

We thank S. Divakaran and D. Hargreaves for helpful discussions. *ARID1A*<sup>-/-</sup> HCT116 cells were a gift from D. Hargreaves (Salk Institute). D. Hargreaves provided ARID1B knockdown constructs. J. Raab (UNC) provided ARID1A knockdown constructs. The Aska-SS and Yamato-SS cell lines were provided by K. Itoh, N. Naka, and S. Takenaka (Osaka University, Japan). E.J.C. was partially supported by an NSF Graduate Research Fellowship and the Ruth L. Kirschstein National Research Service Award (F31 CA203228-02). J.G.K. was partially supported by PHS Grant Number T32 CA09151, awarded by the National Cancer Institute, DHHS. The initial screen and follow-up studies of top inhibitors were supported by NIH grant DA032469 and the Showalter Trust. E.C.D. is supported by The V Foundation for Cancer Research (V2014-004 and D2016-030) and the NIH (CA207532). G.R.C. is supported by NIH grants (CA163915, NS046789), CIRM RB4-05886, SFARI, and the Howard Hughes Medical Institute.

## REFERENCES

- (1) Han, Y., Reyes, A. A., Malik, S., and He, Y. (2020) Cryo-EM Structure of SWI/SNF Complex Bound to a Nucleosome. *Nature* 579 (7799), 452–455.
- (2) Peterson, C. L., and Herskowitz, I. (1992) Characterization of the Yeast SWI1, SWI2, and SWI3 Genes, Which Encode a Global Activator of Transcription. *Cell* 68 (3), 573–583.
- (3) Khavari, P. A., Peterson, C. L., Tamkun, J. W., Mendel, D. B., and Crabtree, G. R. (1993) BRG 1 Contains a Conserved Domain of the SWI 2/SNF 2 Family Necessary for Normal Mitotic Growth and Transcription. *Nature* 366 (6451), 170–174.
- (4) Mashtalir, N., D'Avino, A. R., Michel, B. C., Luo, J., Pan, J., Otto, J. E., Zullow, H. J., McKenzie, Z. M., Kubiak, R. L., St Pierre, R., et al. (2018) Modular Organization and Assembly of SWI/SNF Family Chromatin Remodeling Complexes. *Cell* 175 (5), 1272–1288.
- (5) Hodges, C., Kirkland, J. G., and Crabtree, G. R. (2016) The Many Roles of BAF (mSWI/SNF) and PBAF Complexes in Cancer. *Cold Spring Harbor Perspect. Med.* 6 (8), a026930.
- (6) Mathur, R., Alver, B. H., San Roman, A. K., Wilson, B. G., Wang, X., Agoston, A. T., Park, P. J., Shivdasani, R. A., and Roberts, C. W. M.

(2017) ARID1A Loss Impairs Enhancer-Mediated Gene Regulation and Drives Colon Cancer in Mice. *Nat. Genet.* 49 (2), 296–302.

(7) Lessard, J., Wu, J. I., Ranish, J. A., Wan, M., Winslow, M. M., Staahl, B. T., Wu, H., Aebersold, R., Graef, I. A., and Crabtree, G. R. (2007) An Essential Switch in Subunit Composition of a Chromatin Remodeling Complex during Neural Development. *Neuron* 55 (2), 201–215.

(8) Brownlee, P. M., Meisenberg, C., and Downs, J. A. (2015) The SWI/SNF Chromatin Remodelling Complex: Its Role in Maintaining Genome Stability and Preventing Tumourigenesis. *DNA Repair* 32, 127–133.

(9) Rafati, H., Parra, M., Hakre, S., Moshkin, Y., Verdin, E., and Mahmoudi, T. (2011) Repressive LTR Nucleosome Positioning by the BAF Complex Is Required for HIV Latency. *PLoS Biol.* 9 (11), No. e1001206.

(10) Conrad, R. J., Fozouni, P., Thomas, S., Sy, H., Zhang, Q., Zhou, M.-M., and Ott, M. (2017) The Short Isoform of BRD4 Promotes HIV-1 Latency by Engaging Repressive SWI/SNF Chromatin-Remodeling Complexes. *Mol. Cell* 67 (6), 1001–1012.

(11) Gratkowska-Zmuda, D. M., Kubala, S., Sarnowska, E., et al. (2020) The SWI/SNF ATP-Dependent Chromatin Remodeling Complex in Arabidopsis Responds to Environmental Changes in Temperature-Dependent Manner. *Int. J. Mol. Sci.* 21 (3), 762.

(12) Wu, J. I., Lessard, J., and Crabtree, G. R. (2009) Understanding the Words of Chromatin Regulation. *Cell* 136 (2), 200–206.

(13) Wang, X., Wang, S., Troisi, E. C., Howard, T. P., Haswell, J. R., Wolf, B. K., Hawk, W. H., Ramos, P., Oberlick, E. M., Tzvetkov, E. P., et al. (2019) BRD9 Defines a SWI/SNF Sub-Complex and Constitutes a Specific Vulnerability in Malignant Rhabdoid Tumors. *Nat. Commun.* 10 (1), 1881.

(14) Brien, G. L., Remillard, D., Shi, J., Hemming, M. L., Chabon, J., Wynne, K., Dillon, E. T., Cagney, G., Van Mierlo, G., Baltissen, M. P., et al. (2018) Targeted Degradation of BRD9 Reverses Oncogenic Gene Expression in Synovial Sarcoma. *eLife* 7, No. e41305.

(15) Alpsoy, A., and Dykhuizen, E. C. (2018) Glioma tumor suppressor candidate region gene 1 (GLTSCR1) and its paralog GLTSCR1-like form SWI/SNF chromatin remodeling subcomplexes. *J. Biol. Chem.* 293 (11), 3892–3903.

(16) Gatchalian, J., Malik, S., Ho, J., et al. (2018) A non-canonical BRD9-containing BAF chromatin remodeling complex regulates naive pluripotency in mouse embryonic stem cells. *Nat. Commun.* 9 (1), 5139.

(17) Raab, J. R., Resnick, S., and Magnuson, T. (2015) Genome-Wide Transcriptional Regulation Mediated by Biochemically Distinct SWI/SNF Complexes. *PLoS Genet.* 11 (12), No. e1005748.

(18) Dykhuizen, E. C., Hargreaves, D. C., Miller, E. L., Cui, K., Korshunov, A., Kool, M., Pfister, S., Cho, Y.-J., Zhao, K., and Crabtree, G. R. (2013) BAF Complexes Facilitate Decatenation of DNA by Topoisomerase IIα. *Nature* 497 (7451), 624–627.

(19) Ho, L., Ronan, J. L., Wu, J., et al. (2009) An embryonic stem cell chromatin remodeling complex, esBAF, is essential for embryonic stem cell self-renewal and pluripotency. *Proc. Natl. Acad. Sci. U. S. A.* 106 (13), 5181–5186.

(20) Miller, E. L., Hargreaves, D. C., Kadoch, C., Chang, C.-Y., Calarco, J. P., Hodges, C., Buenrostro, J. D., Cui, K., Greenleaf, W. J., Zhao, K., et al. (2017) TOP2 Synergizes with BAF Chromatin Remodeling for Both Resolution and Formation of Facultative Heterochromatin. *Nat. Struct. Mol. Biol.* 24 (4), 344–352.

(21) Peng, G., Yim, E.-K., Dai, H., Jackson, A. P., van der Burgt, I., Pan, M.-R., Hu, R., Li, K., and Lin, S.-Y. (2009) BRIT1/MCPH1 Links Chromatin Remodelling to DNA Damage Response. *Nat. Cell Biol.* 11 (7), 865–872.

(22) Wang, X., Lee, R. S., Alver, B. H., Haswell, J. R., Wang, S., Mieczkowski, J., Drier, Y., Gillespie, S. M., Archer, T. C., Wu, J. N., et al. (2017) SMARCB1-Mediated SWI/SNF Complex Function Is Essential for Enhancer Regulation. *Nat. Genet.* 49 (2), 289–295.

(23) Yoo, A. S., Staahl, B. T., Chen, L., and Crabtree, G. R. (2009) MicroRNA-Mediated Switching of Chromatin-Remodelling Complexes in Neural Development. *Nature* 460 (7255), 642–646.

- (24) Kadoch, C., Hargreaves, D. C., Hodges, C., Elias, L., Ho, L., Ranish, J., and Crabtree, G. R. (2013) Proteomic and Bioinformatic Analysis of Mammalian SWI/SNF Complexes Identifies Extensive Roles in Human Malignancy. *Nat. Genet.* 45 (6), 592–601.
- (25) Fedorov, O., Castex, J., Tallant, C., Owen, D. R., Martin, S., Aldeghi, M., Monteiro, O., Filippakopoulos, P., Picaud, S., Trzupek, J. D., et al. (2015) Selective Targeting of the BRG/PB1 Bromodomains Impairs Embryonic and Trophoblast Stem Cell Maintenance. *Sci. Adv.* 1 (10), No. e1500723.
- (26) Vangamudi, B., Paul, T. A., Shah, P. K., et al. (2015) The SMARCA2/4 ATPase Domain Surpasses the Bromodomain as a Drug Target in SWI/SNF-Mutant Cancers: Insights from cDNA Rescue and PFI-3 Inhibitor Studies. *Cancer Res.* 75 (18), 3865–3878.
- (27) Muthuswami, R., Mesner, L. D., Wang, D., Hill, D. A., Imbalzano, A. N., and Hockensmith, J. W. (2000) Phosphoamino-glycosides Inhibit SWI2/SNF2 Family DNA-Dependent Molecular Motor Domains. *Biochemistry* 39 (15), 4358–4365.
- (28) Papillon, J. P. N., Nakajima, K., Adair, C. D., Hempel, J., Jouk, A. O., Karki, R. G., Mathieu, S., Möbitz, H., Ntaganda, R., Smith, T., et al. (2018) Discovery of Orally Active Inhibitors of Brahma Homolog (BRM)/SMARCA2 ATPase Activity for the Treatment of Brahma Related Gene 1 (BRG1)/SMARCA4-Mutant Cancers. *J. Med. Chem.* 61 (22), 10155–10172.
- (29) Dykhuizen, E. C., Carmody, L. C., Tolliday, N., Crabtree, G. R., and Palmer, M. A. J. (2012) Screening for Inhibitors of an Essential Chromatin Remodeler in Mouse Embryonic Stem Cells by Monitoring Transcriptional Regulation. *J. Biomol. Screening* 17 (9), 1221–1230.
- (30) Tan, D. S. (2005) Diversity-Oriented Synthesis: Exploring the Intersections between Chemistry and Biology. *Nat. Chem. Biol.* 1 (2), 74–84.
- (31) Kim, S., Chen, J., Cheng, T., Gindulyte, A., He, J., He, S., Li, Q., Shoemaker, B. A., Thiessen, P. A., Yu, B., et al. (2019) PubChem 2019 Update: Improved Access to Chemical Data. *Nucleic Acids Res.* 47 (D1), D1102–D1109.
- (32) Marian, C. A., Stoszko, M., Wang, L., Leighty, M. W., de Crignis, E., Maschinot, C. A., Gatchalian, J., Carter, B. C., Chowdhury, B., Hargreaves, D. C., et al. (2018) Small Molecule Targeting of Specific BAF (mSWI/SNF) Complexes for HIV Latency Reversal. *Cell Chem. Biol.* 25 (12), 1443–1455.
- (33) Michel, B. C., D'Avino, A. R., Cassel, S. H., Mashtalir, N., McKenzie, Z. M., McBride, M. J., Valencia, A. M., Zhou, Q., Bocker, M., Soares, L. M. M., et al. (2018) A Non-Canonical SWI/SNF Complex Is a Synthetic Lethal Target in Cancers Driven by BAF Complex Perturbation. *Nat. Cell Biol.* 20 (12), 1410–1420.
- (34) Shiloh, Y., and Ziv, Y. (2013) The ATM Protein Kinase: Regulating the Cellular Response to Genotoxic Stress, and More. *Nat. Rev. Mol. Cell Biol.* 14 (4), 197–210.
- (35) Zou, L., Liu, D., and Elledge, S. J. (2003) Replication Protein A-Mediated Recruitment and Activation of Rad17 Complexes. *Proc. Natl. Acad. Sci. U. S. A.* 100 (24), 13827–13832.
- (36) Stoszko, M., De Crignis, E., Rokx, C., Khalid, M. M., Lungu, C., Palstra, R.-J., Kan, T. W., Boucher, C., Verbon, A., Dykhuizen, E. C., et al. (2016) Small Molecule Inhibitors of BAF: A Promising Family of Compounds in HIV-1 Latency Reversal. *EBioMedicine* 3, 108–121.
- (37) Karnitz, L. M., and Zou, L. (2015) Molecular Pathways: Targeting ATR in Cancer Therapy. *Clin. Cancer Res.* 21 (21), 4780–4785.
- (38) Weber, A. M., and Ryan, A. J. (2015) ATM and ATR as Therapeutic Targets in Cancer. *Pharmacol. Ther.* 149, 124–138.
- (39) Williamson, C. T., Miller, R., Pemberton, H. N., Jones, S. E., Campbell, J., Konde, A., Badham, N., Rafiq, R., Brough, R., Gulati, A., et al. (2016) ATR Inhibitors as a Synthetic Lethal Therapy for Tumours Deficient in ARID1A. *Nat. Commun.* 7, 13837.
- (40) Weber, C. M., Hafner, A., Braun, S. M. G., Boettiger, A. N., and Crabtree, G. R. (2020) mSWI/SNF Promotes Distal Repression by Titrating Polycomb Dosage. *bioRxiv*, <https://doi.org/10.1101/2020.01.29.925586> (accessed April 1, 2020).
- (41) Chou, T.-C. (2006) Theoretical Basis, Experimental Design, and Computerized Simulation of Synergism and Antagonism in Drug Combination Studies. *Pharmacol. Rev.* 58 (3), 621–681.
- (42) Chou, T.-C. (2010) Drug Combination Studies and Their Synergy Quantification Using the Chou-Talalay Method. *Cancer Res.* 70 (2), 440–446.
- (43) Chou, T. C., and Talalay, P. (1984) Quantitative Analysis of Dose-Effect Relationships: The Combined Effects of Multiple Drugs or Enzyme Inhibitors. *Adv. Enzyme Regul.* 22, 27–55.
- (44) Brownlee, P. M., Chambers, A. L., Cloney, R., Bianchi, A., and Downs, J. A. (2014) BAF180 Promotes Cohesion and Prevents Genome Instability and Aneuploidy. *Cell Rep.* 6 (6), 973–981.
- (45) Chowdhury, B., Porter, E. G., Stewart, J. C., Ferreira, C. R., Schipma, M. J., and Dykhuizen, E. C. (2016) PBRM1 Regulates the Expression of Genes Involved in Metabolism and Cell Adhesion in Renal Clear Cell Carcinoma. *PLoS One* 11 (4), No. e0153718.
- (46) Jiao, Y., Pawlik, T. M., Anders, R. A., Selaru, F. M., Streppel, M. M., Lucas, D. J., Niknafs, N., Guthrie, V. B., Maitra, A., Argani, P., et al. (2013) Exome Sequencing Identifies Frequent Inactivating Mutations in BAP1, ARID1A and PBRM1 in Intrahepatic Cholangiocarcinomas. *Nat. Genet.* 45 (12), 1470–1473.
- (47) Macher-Goeppinger, S., Keith, M., Tagscherer, K. E., Singer, S., Winkler, J., Hofmann, T. G., Pahernik, S., Duensing, S., Hohenfellner, M., Kopitz, J., et al. (2015) PBRM1 (BAF180) Protein Is Functionally Regulated by p53-Induced Protein Degradation in Renal Cell Carcinomas. *J. Pathol.* 237 (4), 460–471.
- (48) Kwon, S.-J., Park, J.-H., Park, E.-J., Lee, S.-A., Lee, H.-S., Kang, S. W., and Kwon, J. (2015) ATM-Mediated Phosphorylation of the Chromatin Remodeling Enzyme BRG1 Modulates DNA Double-Strand Break Repair. *Oncogene* 34 (3), 303–313.
- (49) Gao, H., Huang, K.-C., Yamasaki, E. F., Chan, K. K., Chohan, L., and Snapka, R. M. (1999) XK469, a Selective Topoisomerase II $\beta$  Poison. *Proc. Natl. Acad. Sci. U. S. A.* 96 (21), 12168–12173.
- (50) Fillmore, C. M., Xu, C., Desai, P. T., Berry, J. M., Rowbotham, S. P., Lin, Y.-J., Zhang, H., Marquez, V. E., Hammerman, P. S., Wong, K.-K., et al. (2015) EZH2 Inhibition Sensitizes BRG1 and EGFR Mutant Lung Tumours to TopoII Inhibitors. *Nature* 520 (7546), 239–242.
- (51) Pang, B., de Jong, J., Qiao, X., Wessels, L. F. A., and Neeffes, J. (2015) Chemical Profiling of the Genome with Anti-Cancer Drugs Defines Target Specificities. *Nat. Chem. Biol.* 11 (7), 472–480.
- (52) Kelso, T. W. R., Porter, D. K., Amaral, M. L., Shokhirev, M. N., Benner, C., and Hargreaves, D. C. (2017) Chromatin Accessibility Underlies Synthetic Lethality of SWI/SNF Subunits in ARID1A-Mutant Cancers. *eLife* 6, No. e30506.
- (53) Helming, K. C., Wang, X., Wilson, B. G., Vazquez, F., Haswell, J. R., Manchester, H. E., Kim, Y., Kryukov, G. V., Ghandi, M., Aguirre, A. J., et al. (2014) ARID1B Is a Specific Vulnerability in ARID1A-Mutant Cancers. *Nat. Med.* 20 (3), 251–254.
- (54) Kadoch, C., and Crabtree, G. R. (2015) Mammalian SWI/SNF Chromatin Remodeling Complexes and Cancer: Mechanistic Insights Gained from Human Genomics. *Sci. Adv.* 1 (5), No. e1500447.
- (55) Pan, D., Kobayashi, A., Jiang, P., de Andrade, L. F., Tay, R. E., Luoma, A. M., Tsoucas, D., Qiu, X., Lim, K., Rao, P., et al. (2018) A Major Chromatin Regulator Determines Resistance of Tumor Cells to T Cell-mediated Killing. *Science* 359 (6377), 770–775.
- (56) Kadoch, C., and Crabtree, G. R. (2013) Reversible disruption of mSWI/SNF (BAF) complexes by the SS18-SSX oncogenic fusion in synovial sarcoma. *Cell* 153 (1), 71–85.
- (57) Roberts, C. W., Galusha, S. A., McMenamin, M. E., Fletcher, C. D., and Orkin, S. H. (2000) Haploinsufficiency of Snf5 (integrase Interactor 1) Predisposes to Malignant Rhabdoid Tumors in Mice. *Proc. Natl. Acad. Sci. U. S. A.* 97 (25), 13796–13800.
- (58) Wilson, B. G., Wang, X., Shen, X., McKenna, E. S., Lemieux, M. E., Cho, Y.-J., Koellhoffer, E. C., Pomeroy, S. L., Orkin, S. H., and Roberts, C. W. M. (2010) Epigenetic Antagonism between Polycomb and SWI/SNF Complexes during Oncogenic Transformation. *Cancer Cell* 18 (4), 316–328.

- (59) Marcaurelle, L. A., Comer, E., Dandapani, S., Duvall, J. R., Gerard, B., Kesavan, S., Lee, M. D., 4th, Liu, H., Lowe, J. T., Marie, J.-C., et al. (2010) An Aldol-Based Build/couple/pair Strategy for the Synthesis of Medium- and Large-Sized Rings: Discovery of Macrocyclic Histone Deacetylase Inhibitors. *J. Am. Chem. Soc.* 132 (47), 16962–16976.
- (60) Tiscornia, G., Singer, O., and Verma, I. M. (2006) Design and Cloning of Lentiviral Vectors Expressing Small Interfering RNAs. *Nat. Protoc.* 1 (1), 234–240.